An Efficient Method for the Determination of the Probability of Failure on the Basis of LCF Data: Application to Turbogenerator Design

G. Olmi[1]

Abstract: Turbogenerator rotors and coil retaining rings are highly loaded components, under low cycle fatigue at every machine switch on and switch off transient. Their failure during service may lead to very serious consequences. The present paper utilizes several experimental data, concerning the static, cyclic and fatigue behaviour of the rotor material, in order to perform a probabilistic analysis. All the main methodological issues are tackled, consisting in the experimental data processing, in the choice of the random variables that are involved in the fatigue process, in the determination of their distributions, in the practical computation of the probability of failure and of the safety index in the machine life range. The here implemented numerical method has remarkable properties to be emphasized: low computational times, generality of application, and accuracy. In order to test the method for accuracy, the obtained results were validated by a comparison with those of a Monte Carlo simulation and with reference data reported in the current literature.

Keywords: Low Cycle Fatigue (LCF), Turbogenerator rotor, Advanced Mean Value (AMV) Method, Failure Probability, Safety Index.

1 Introduction

A turbogenerator, in particular its main components, the rotor and the coil retaining ring (CRR), is typically subjected to a low cycle fatigue (LCF) load, with detailed information contained in previous contributions by the author [Olmi and Freddi (2009); Olmi and Freddi (2010)]. LCF load can be explained as follows: turbogenerators are designed for energy production at a constant rotational speed (3,000 rpm, increased up to 3,600 rpm in pretrial conditions), consequently the centrifugal force acting on rotating devices maintains a constant value in steady-state conditions, i.e. it is a static force. The result is that the stress and strain states also

---

[1] DIEM Department, University of Bologna, Italy, e-mail: giorgio.olmi@unibo.it.

have a constant value during rotation at a constant speed. When the machine is switched off, its speed is gradually lowered, with the consequence that the centrifugal force is decreased and the related states of load experience a variation. The final outcome is that both the rotor and the CRR experience LCF cycles during the machine switch ons and switch offs. The present paper is focused on the rotor: this component, having 1.2 m diameter and 4.5 m length exhibits uniformly spaced longitudinal slots. Copper conductors and insulating materials are packed into the slots and emerge at their ends, to join the circumferential arc portion of the windings to form a coil, which is wound around the rotor. As the rotor spins, the copper conductors are subjected to high centrifugal forces and must be restrained. Along most of the rotor length, this resistant is provided by non-magnetic metal wedges applied along the slots. At the ends, due to the coil emersion to the surface, wedges cannot be applied and constraining is achieved by the assembly of CRRs that are shrunk fitted onto the rotor body over the coils. The interference coupling generates tangential and radial stresses, acting both on the rotor and on the CRRs, with the first ones being greater than the second ones. The CRR is fixed by locking keys against displacements in the axial direction, which implies the generation of additional stresses along this direction. However, these loads are of a small entity and about one order of magnitude lower than those in the tangential and radial directions. The stresses generated on the rotor during shrink fitting are released as the rotor starts to spin, and increased again, when rotation is stopped. Consequently, a cycle is completed after each switch on and switch off: according to the actual energetic policies, the expected number of cycles in the whole machine life is ranging between 10,000 and 15,000. It is worth mentioning to observe that the rotor is subjected to rotating bending: this type of load can be regarded as a high cycle fatigue load, with one cycle being completed at each rotation. However, due to the high radial dimensions, the entity of the generated stresses is very low and negligible with respect to the previously mentioned ones.

The consequences of an on service failure involving the rotor or the CRR may be very serious, since an explosion and resultant fire are likely to occur. Such an occurrence could lead to fracture of the shaft line, breakage of lubrication oil pipe lines, resulting in a catastrophic failure of the whole turbogenerator. An image of an exploded rotor is shown in Fig. 1, while other similar incidents are reported in [Skorchelletty, Silina, Zaytsev, Maslov and Lubeznova (1981); Speidel (1981); Kilpatrick and Schneider (1988)].

As exposed in some references, e.g. [Apostolakis (1990); Huang and Du (2008)] the performance of an engineered system is often affected by several uncertainties. Should the designer fail in a full comprehension of the involved variables, regarding the product or the device being developed, a lack of the final quality or unexpected
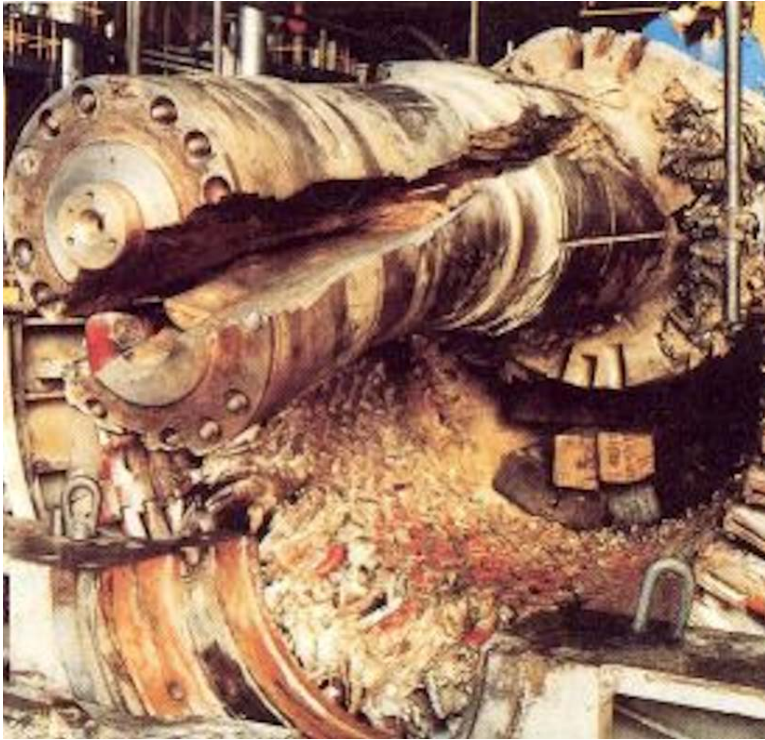
Figure 1: Rotor failure resulting in its explosion

failures could occur. Being able to manage and estimate the effects of uncertainty on the design performance, by running probabilistic analyses based on the experimental knowledge of the structural behaviour is rapidly spreading in industry [Haldar and Mahadevan (2001); Du and Chen (2000); Mailhot and Villeneuve (2003); Seo and Kwak (2002); Putko, Newman, Taylor III and Green (2002); Nikolaidis, Chen, Cudney, Hatftka and Rosca (2004)]. The execution of a reliability quantitative analysis is nowadays more and more important: for instance, it is important that turbogenerator design, usually performed by conventional deterministic structural calculation, is supported by a careful study of the probability of failure in the entire machine life range.

The aforementioned analysis can be implemented as follows. Let $\underline{U}$ be the vector of the r input variables U_i. Thus, we have $\underline{U} = [U_1, \ldots, U_r]^T$, while the output variable is usually indicated by Y. In the present study the input variables, with experimentally investigated distributions, are referred to material properties. They can be regarded as random variables [Huang and Du (2008)], being subjected to

fluctuations due to several causes (environmental conditions, different material lots, ...). The output variable is usually related to the device structural response: in the present study it represents the expected life. Let g be the functional relationship between the effect Y and its causes $\underline{U}$: $Y = g(\underline{U})$. The goal of the probabilistic analysis consists in the determination of the probability P of $Y \leq y$, given the distributions of the random inputs and being y a threshold value.

The present study is going to investigate the probability that the computed rotor life is lower than design requirements (represented by y), related to the expected number of switch ons and switch offs. When the $Y \leq y$ condition is satisfied, a failure is likely to occur, thus the P probability has the meaning of a failure probability. The specific case when the equality $Y = y$ is verified, indicates that the computed life is coincident with design minimum requirements, without any safety margin. In other words, failure should occur exactly at the end of the expected life, e.g. at 15,000 cycles. For this reason, the condition $Y = y$ is usually regarded as the limit state, at the boundary between the "failure" and "performance" conditions or the "safe" and "unsafe" domains. From the mathematical point of view it corresponds to the roots of the failure function $h(\underline{U}) = Y - y = 0$.

Theoretically, the cumulative distribution function (CDF) of Y, F_Y can be calculated by computing a multi-dimensional integral, Eq. 1.

$$F_Y(y) = P(Y \leq y) \int\limits_{Y=g(\underline{U}) \leq y} f_{\underline{U}}(\underline{U}) \tag{1}$$

The term $f_U(\underline{U})$ is the joint probability density function of the random variable vector, whose components are presumed to be mutually independent. In practice, the complexity of the integration domain, having nonlinear boundaries, and the high dimensionality make it impossible to obtain a closed form analytical solution to the probability integration in Eq. 1.

Alternative methods must therefore be used for probabilistic uncertainty analysis. The first approaches were performed by the Monte Carlo method (MC), having the advantage of being quite easy from the conceptual point of view. However, this sampling method has the serious drawback of being computationally expensive and inefficient for problems where high reliability and complicated functional relationships between the output and the inputs are involved. It must be remarked that many engineering problems, like that under study, have very high reliability, moreover, in some cases, it is not possible to express the g relationship in a closed form [Huang and Du (2008); Wang and Grandhi (1996); Wirsching, Torng and Martin (1991)].

In order to overcome these difficulties, approximated numerical methods were de-

veloped. The first one to be cited is the mean value first-order second-moment method (MVFOSM), which introduced the use of first order Taylor expansions to achieve a suitable approximation of the *g* or *h* functions at the mean values of random variables, presumed to be normally distributed [Haldar and Mahadevan (2001); Cornell (1969)]. Despite its good efficiency, the MVFOSM method has a lower accuracy than that of sampling methods, such as the MC. This lack in accuracy is due to the expansion procedure, which is performed in the neighbourhood of a specific and static point, defined by the mean values of the random variables. Moreover, it can be shown that different, but analytically equivalent, formulations of the same failure function may lead to very different quantitative estimations of the reliability properties [Wang and Grandhi (1996)].

The mentioned drawbacks were overcome by [Hasofer and Lind (1974)], who introduced the procedure of variable reduction and the computation of a safety index, being now independent of the analytical formulation and being strictly related to the entity of failure probability. A further improvement, which made it possible to get a good balance between efficiency and accuracy, consisted in the development of Most Probable Point (MPP)-based methods. An upgrade of the MVFOSM led to the introduction of the advanced first-order second-moment method (AFOSM): this methodology also utilizes the Taylor series tool, but expansion is performed at an iteratively determined point, called "design point" or "most probable failure point (MPP)". This point is defined by the values of the random variables satisfying the equation $h(\underline{U}) = 0$, and being at the same time as close as possible to the aforementioned mean values. From the geometrical point of view, the "most probable failure point" lies on the failure function separating the safe and unsafe domains, and is univocally determined, for being at the minimum distance from the point corresponding to the average values of the inputs. In other words, the design point corresponds to the maximum likelihood of failure occurrence.

The previous methods were extended by Rackwitz and Fiessler [Rackwitz and Fiessler (1978)] to non normally distributed random variables. The first order reliability method (FORM) [Breitung (1984)] is based on the same concept of failure function expansion in the neighbourhood of the design point. FORM is more efficient than sampling-based ones, but is computationally expensive; moreover, it cannot be applied or its results may be questionable, when the *g* or *h* functions are analytically complicated or not available in a closed form. In case of significant non linearities of the studied system around the design point, the aforementioned method could fail to converge to an acceptable result [Ebbeler, Newlin and Grigoriu (1995)]. Nowadays, the mostly used methods [Che (2008)] are the AFOSM, the mean-value first order Saddlepoint Approximation (MVFOSA) [Huang and Du (2008)] and the Advanced Mean Value (AMV) [Wu, Millwater and Cruse (1990)].

The last one combines most of the main advantages of the previously cited methods and is highly efficient and accurate.

The analysis of literature concerned with turbines and turbogenerators showed that, despite the serious consequences of a failure and the importance of estimating its probability of occurrence, very few practical applications are described. Some examples in close fields are reported in [Liu, Lu, Xu and Yue (2005); Avrithi and Ayyub (2010)]: they regard applications to aeronautical engine turbines and to nuclear piping design, but no details are provided about the determination of random variable distributions.

The AMV method is often cited as a suitable tool for the development of the probabilistic analysis [Wu and Wirsching (1984)], but a detailed description of the analytical steps to be followed as a general procedure is missing. In particular, the main steps are the following: the determination of the Taylor expansion and of the failure function, coordinate reduction, the computation of the design point, of the safety index and of the probability of failure. In addition, the integration of LCF data with reliability calculation still needs investigations. The question of the extrapolation of the random variables and related distributions from the experimental results is not tackled anywhere. Finally, the iterative procedure must be carefully implemented and improved in order to match both efficiency and accuracy.

The subject of the present paper consists in the determination of the safety index and of the probability of failure of the previously described turbogenerator rotor. This study considers failures due to LCF cracking at the shrink-fit coupling zone on the rotor, since it is the most critical failure mode. The two aforementioned parameters are computed at different stages in the machine life, in order to finally determine the CDF of the expected life. The calculation is performed by combining experimental data [Olmi and Freddi (2010)], related to the static, cyclic and fatigue curves of the involved material, with information regarding the local stress and strain states and with suitable numerical tools for reliability analyses. From the methodological point of view, full details are provided on the applied numerical procedure, based on the AMV method, for probabilistic computation. Particular emphasis is given to the processing of the experimental data for the determination of random variable distributions, while also the iterative procedure is carefully implemented.

Finally, it must be remarked that, despite the non linearity of the material curves, the here applied model operates a linearization in the neighbourhood of the MPP. A further aim is to show that, in case of non strong non linearities, a linear model also is able to provide accurate results, with a positive outcome in terms of computational efficiency. This good behaviour of the linear models is confirmed also by [Haldar and Mahadevan (2001); Huang and Du (2008); Youn and Choi (2004);

Du, Sudjianto and Chen (2004); Du and Chen (2004); Youn and Choi (2004); Hohenbichler, Gollwitzer, Kruse and Rackwitz (1987); Thoft-Christensen and Baker (1982)].

2   Materials and Methods

2.1   *Static, cyclic and LCF curves: analytical coefficients and related tolerance bands*

In the previous stage of the current research [Olmi and Freddi (2010)] we determined the fatigue curves of a material, 26 NiCrMoV 14 5, which is typically used for the manufacturing of turbogenerator rotors. The experimental characterization was carried out by testing specimens machined in the tangential and radial directions from blanks of trial rotors. The choice of these directions was supported by previous experimental studies reported in literature [Orita, Ikeda, Iwadate and Ishizaka (1990); Balitskii, Krohmalny and Ripey (2000)]. In addition, it was observed that the states of stress and strain are much greater along the tangential and radial direction rather than in the longitudinal direction (see also Paragraph 1). Furthermore, in [Olmi and Freddi (2010); Olmi (2012)] a suitable statistical model, based on the Analysis of Variance [Berger and Maurer (2002)], was developed to investigate on the significance of the differences between the determined curves in the tangential and radial directions. These differences resulted to be not significant with respect to the experimental uncertainty (they may be regarded within the experimental uncertainty of fatigue tests). Based on this conclusion, it was finally decided to consider the characterization data in the tangential direction, i.e. in the direction where the highest stresses are usually generated in shrunk-fitted axial symmetric components.

In [Olmi and Freddi (2010)] the fatigue strength (σ'_f) and fatigue ductility (ε'_f) coefficients, together with related exponents (b, c) for the analytical description of the Manson-Coffin curve were determined in agreement with the ISO Standard [ISO 12106 (2003)]. In particular, the total strain amplitude was decomposed into its elastic and plastic parts (respectively, subscripts $_{el.}$ and $_{pl.}$) and linear regressions were performed in the logarithmic scale (Eqs. 2-4).

$$\frac{\Delta\varepsilon}{2} = \frac{\Delta\varepsilon_{el.}}{2} + \frac{\Delta\varepsilon_{pl.}}{2} = \frac{\sigma'_f}{E}(2N)^b + \varepsilon'_f(2N)^c \qquad (2)$$

$$Lg\left(\frac{\Delta\varepsilon_{el.}}{2}\right) = Lg\left(\frac{\sigma'_f}{E}\right) + b \cdot Lg(2N) \qquad (3)$$

$$Lg\left(\frac{\Delta\varepsilon_{pl.}}{2}\right) = Lg\left(\varepsilon'_f\right) + c \cdot Lg(2N) \qquad (4)$$

A suitable statistical model [Doyle (2004)] made it possible to determine the standard deviations of the constant terms and of the slopes of the regressions. It can be observed that the estimation of the standard deviations leads to the determination of the Normal distributions of Lg(σ'_f), Lg(ε'_f), b and c, as the Young's modulus E is usually [Wirsching, Torng and Martin (1991); Wu and Wirsching (1984)] regarded as a deterministic constant. The adoption of Log-Normal distributions for the fatigue strength and fatigue ductility coefficients (σ'_f and ε'_f), and of Normal distributions for the exponents b and c is in agreement with the assumptions in [Wirsching, Torng and Martin (1991); Wu and Wirsching (1984)]. This is an interesting outcome of the result analysis, especially for two reasons. First of all, as reported in [Olmi and Freddi (2010)], by using the basic properties of the Gaussian distributions it is possible to determine tolerance ranges at the 95.5% confidence level to be applied to each coefficient. Furthermore, from the graphical point of view it is possible to determine lower and upper bounds to be applied to the LCF curve, which take the "worst scenario of twice the standard deviation" into account. These two bound curves, wrapped around the nominal fatigue curve, enclose a confidence band where the real fatigue curve is likely to be located. The lower bound is determined for all the coefficients having the lowest values of the tolerance range, while the upper one is determined for the highest ones. On the other hand, the conducted statistical analysis is an essential step towards the reliability analysis detailed in Paragraphs 2.2-2.4. Fig. 2 shows the Manson-Coffin curve of the rotor material characterized in the tangential direction together with its lower and upper bounds.

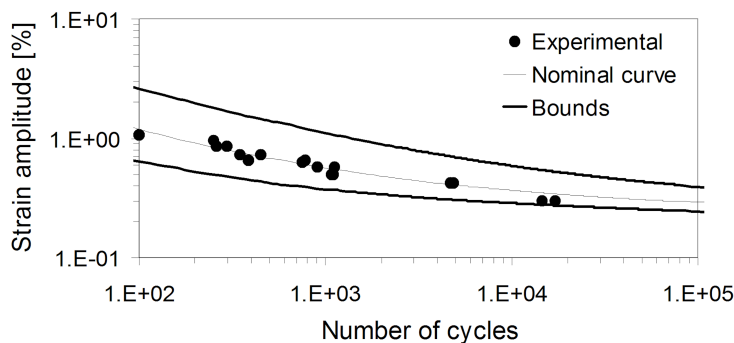One of the mostly used stress-strain functional relationships in the analytical de-

Figure 2: Manson-Coffin curve of the rotor material together with its tolerance band

scription of the static and cyclic curves, is the Ramberg-Osgood model. Its coefficients, namely the static and cyclic coefficients of plasticity (K, K') and the related hardening exponents (n, n') can be determined by a similar procedure of linear interpolation in the logarithmic scale. A sample of the required processing is shown in Eqs. 5-6, with reference to the static curve: in particular, the function in Eq. 6 may be regarded as a straight line in the variables [$Lg(\varepsilon_{pl.})$, $Lg(\sigma)$].

$$\varepsilon = \varepsilon_{el.} + \varepsilon_{pl.} = \frac{\sigma}{E} + \left(\frac{\sigma}{K}\right)^{\frac{1}{n}} \tag{5}$$

$$Lg\left(\varepsilon_{pl.}\right) = \frac{1}{n}Lg\left(\sigma\right) - \frac{1}{n}\cdot Lg\left(K\right) \Leftrightarrow Lg\left(\sigma\right) = n\cdot Lg\left(\varepsilon_{pl.}\right) + Lg\left(K\right) \tag{6}$$

As a consequence, the cited statistical model [Doyle (2004)] may be applied for the estimation of the standard deviations of its slope and constant term. The knowledge of the mean values and of the standard deviations leads to the determination of the Normal distributions of the slopes and constant terms, being related to the hardening exponents (n, n') and to the coefficients of plasticity (K, K') respectively. Again, by using the basic properties of Normal distributions, it is possible to determine tolerance ranges for the aforementioned coefficients and lower and upper bounds to be applied to the static and cyclic curves. The determined curves for the rotor material with bands accounting for the "worst scenario of twice the standard deviation" are shown in Fig. 3. It must be remarked that the variation bands include just the plasticity related parts of the two curves. It is due to the aforementioned hypothesis of considering the Young's modulus E as a deterministic constant.

2.2 *Mathematical model for the determination of the local stress-strain states and for life prediction*

The experimentally determined static, cyclic, LCF curves and related analytical equations make it possible to simulate the stress-strain hysteresis loops at the most critical locations in the neighborhood of the rotor coupling surface onto which the CRR is shrunk fitted (highlighted in Fig. 4).

The local states of load can therefore be monitored at the main turbogenerator life stages: from assembly to regular use at the steady-state rotational speed. The problem is initially approached from the deterministic point of view, considering the analytical expressions of the static, cyclic and fatigue curves for the nominal values of the involved coefficients. The simulation of the stress-strain hysteresis loops is performed by applying the Neuber's hyperbola model in the determination of tip points. The obtained loops, are depicted in Fig. 5 and can be described as in the following:
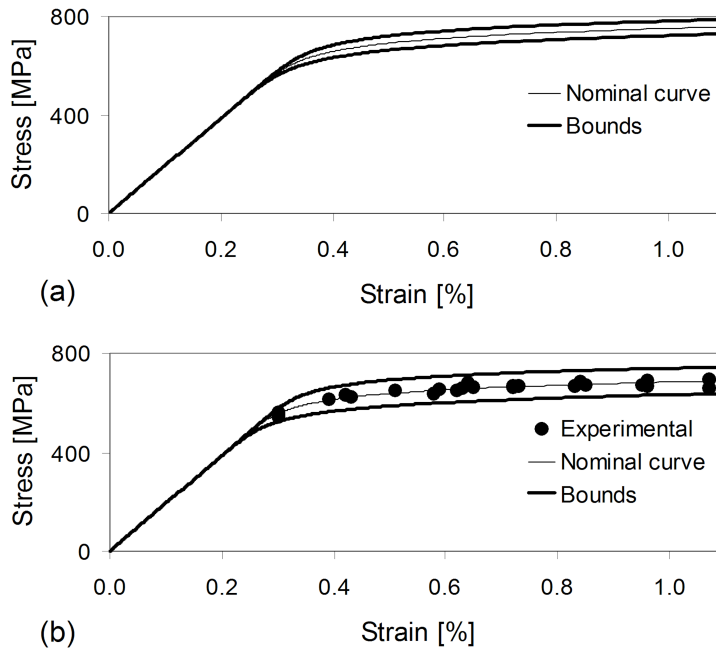
Figure 3: Static (a) and cyclic (b) curves of the rotor material together with related tolerance bands

Curve 0-1: compression of rotor upon shrink-fit during machine assembly. Compression stresses act both along the radial and the tangential directions.

Cycle 1-2-3: machine pretesting at a 20% increased rotational speed (3,600 rpm, point 2) and following stop (point 3). During rotation, the centrifugal force tends to eject the copper coils, which are restrained by the CRR: as a consequence the CRR swells in tension and the compression stresses are released. Despite the nominal state of compression, a local state of tension may occur due to the Bauschinger effect (point 2). Afterwards, the speed is lowered down to zero upon machine switch off (point 3). This loop is repeated only once during machine pre-trial.

Cycle 3-4-5: Machine starting and speed increase up to the nominal value of 3,000 rpm (point 4); speed decrease down to zero, as the machine is switched off (point 5). This last cycle corresponds to the typical use of the turbogenerator, rotating at its nominal speed with about 10,000-15,000 transients, as explained in Paragraph 1.

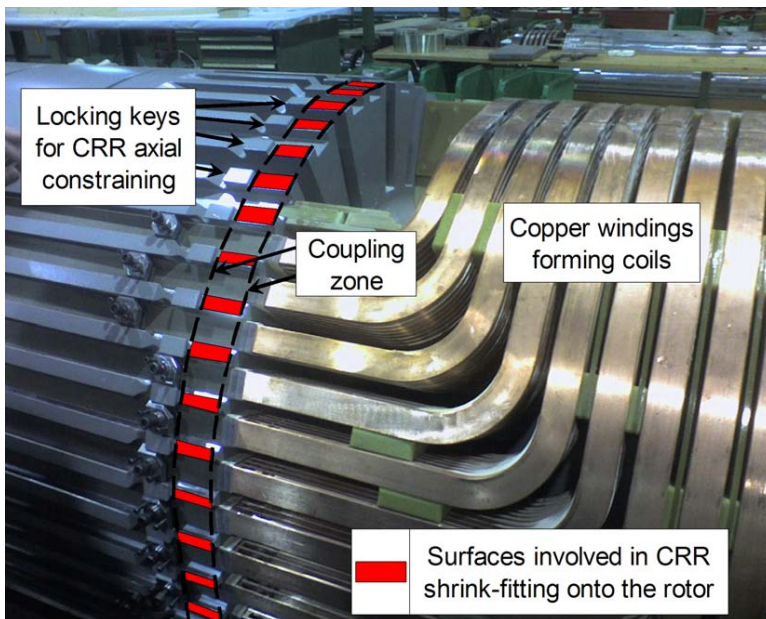The tip points can be determined by solving the two-equation system in Eq. 7,

Figure 4: A photo of the turbogenerator rotor, where the coupling surfaces are highlighted
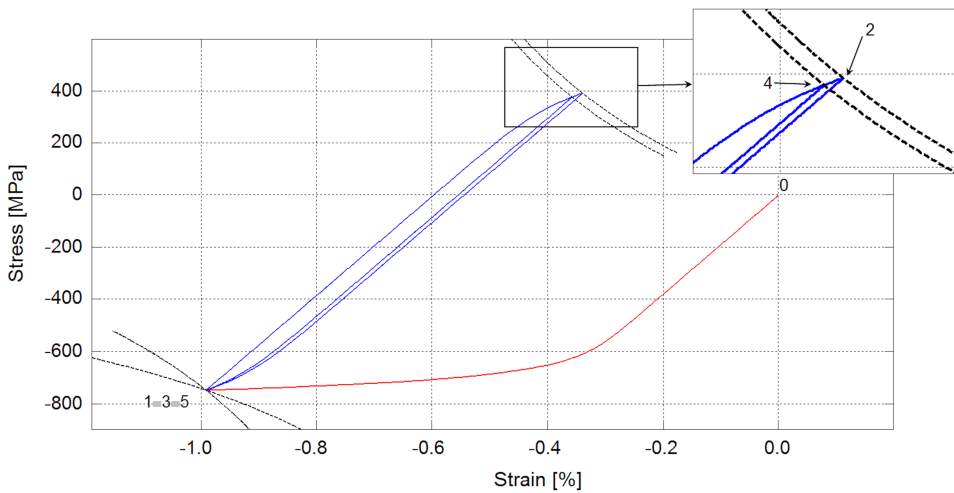

Figure 5: Stress-strain hysteresis loops at the most critical location of the rotor shrink-fit section
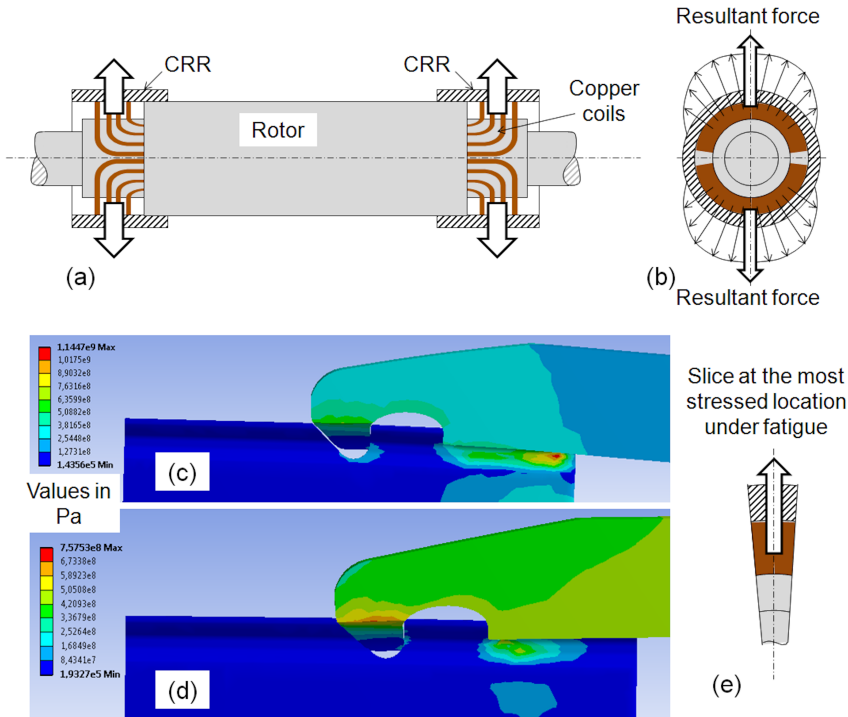
Figure 6: A scheme of the rotor-CRR coupling and of the centrifugal forces transmitted by copper coils (a, b), Von Mises stress field in the off condition (c) and at the speed of 3,000 rpm (d) and a scheme of the simulated slice (e)

consisting in the analytical description of the hysteresis loop branch in its steady-state condition and in the Neuber's hyperbola. The term Δ indicates stress and strain ranges. In the case of the tip point 1, the static curve, with the analytical expression reported in Eq. 5, must be used. It can be observed that the analytical expression of the hysteresis loop branch, contains the terms K' and n', i.e., the previously mentioned coefficients of the cyclic curve. The expression in the first row of Eq. 7 is based on the 2:1 homothetic relationship between the trends of the hysteresis loop branches and of the cyclic curve for Masing materials. The adopted hardening model in the plastic field takes the Bauschinger effect into account and can therefore be regarded within the "kinematic hardening" models. It must be argued that the stress and strain states are multi-axial, with components along the

tangential and radial directions.

$$
\begin{cases}
\frac{\Delta\varepsilon}{2} = \frac{\Delta\sigma}{2E} + \left(\frac{\Delta\sigma}{2K'}\right)^{\frac{1}{n'}} \\
\Delta\sigma \cdot \Delta\varepsilon = \frac{(K_T \cdot \Delta S)^2}{E} = \Delta\sigma_{el.} \cdot \Delta\varepsilon_{el.}
\end{cases}
\tag{7}
$$

In order to extend Eq. 7 to the multi-axial stress condition, the equivalent criterion of Von Mises stress and strain is adopted here, so equivalent Von Mises stress and strain amplitudes must be considered. It can be justified by observing that all the stress-strain components experience cyclic variations that are all in phase; moreover, it is a common approximation in the study of the LCF performance of complexly shaped devices [Liu, Lu, Xu and Yue (2005); Suresh (1991)].

The stress concentration coefficient, K_T, in the second equation, cannot be correctly defined for not-beam components, but the constant term of the hyperbolic distribution can be easily estimated by the computation of the stress and strain ranges ($\Delta\sigma_{el.}$, $\Delta\varepsilon_{el.}$), considering a linear elastic model. They can be regarded as the nominal state of load and can be easily computed, by running FEM simulations in the elastic field, considering the two limit conditions of shrink-fit with zero rotational speed and of shrink-fit combined to the actual value of speed, 3,600 rpm in the pretrial conditions and 3,000 in the conventional use. A scheme of the rotor-CRR coupling and of centrifugal loads during rotation is shown in Fig. 6 (a, b). The resulting state of stress is reported in its lower part (Fig. 6 (c, d)), with reference to the conditions of not rotating machine and of the nominal speed of 3,000 rpm. According to the aforementioned scheme, the simulation refers to a slice (Fig. 6 (e)) of the coupling, corresponding to the angular location, where the stress and strain states experience their maximum amplitude variations.

Finally, the last item, concerning life estimation, is tackled using the experimentally determined fatigue curve. The Manson – Coffin strain-life model is usually applied for structures under LCF. Its conventional formulation, reported in Eq. 2 can be modified, Eq. 8, to take the effects of mean stress and mean strain on the fatigue life into consideration [Dowling (2006)].

$$
\frac{\Delta\varepsilon}{2} = \frac{\sigma'_f - \sigma_m}{E}(2N)^b + \left(\varepsilon'_f - \varepsilon_m\right)(2N)^c
\tag{8}
$$

The terms σ_m and ε_m must be respectively regarded as the mean of Von Mises equivalent stress and as the mean of Von Mises equivalent strain. However, some observations are needed with reference to the plastic term in Eq. 8. In the present case, according to experimental results in [Olmi and Freddi (2010)], $\varepsilon'_f = 0.13$, while ε_m (see Fig. 5), is approximately between $-0.7 \cdot 10^{-2}$ and $-0.6 \cdot 10^{-2}$. In the performed life computation the mean strain term is neglected for two reasons. First

of all, based on the data above, it is about two orders of magnitude lower than ε'_f. Secondly, in many references it is reported that there is little or no effect of mean stresses and strains in the plastic part of the Manson-Coffin curve, as large amounts of plastic deformation usually eradicate any beneficial or detrimental effect of a mean stress-strain, due to its relaxation [ASM International Handbook Committee (1996); Bannantine, Comer and Handrock (1990); Ellyin (1997)]. Consequently, closed loop life estimation is here conducted according to Eq. 9, where the mean stress correction is applied to the elastic term only.

$$\frac{\Delta\varepsilon}{2} = \frac{\sigma'_f - \sigma_m}{E}(2N)^b + \varepsilon'_f(2N)^c \qquad (9)$$

The relationship in Eq. 9 is commonly regarded as the modified Morrow approach and was successfully used in similar applications, involving steels for turbine disks or blades, for instance in [Liu, Lu, Xu and Yue (2005); Vyas, Sidharth and Rao (1997)]. In other papers, such as in [Wu and Wirsching (1984)], the mean stress term was completely neglected (even in the elastic term), due to the aforementioned stress relaxation effect.

From the operative point of view, life estimation up to crack initiation is conducted by applying Eq. 9 to the two closed loops (cycles 1-2-3 and 3-4-5) in Fig. 5 and by the following application of a cumulative damage theory (the Palmgren-Miner model).

2.3   *Choice of the random variables and resume of the considered distributions*

The mathematical model described above was used to tackle the problem for the probabilistic point of view, with the final goal of the determination of the CDF of the rotor life. The first step consisted in a discussion regarding the variables having an impact on the life, in order to establish whether they should be regarded as random variables or as deterministic parameters. In particular, the discussion dealt with the opportunity of considering the nominal state of load at the most critical location of shrink-fit ($\Delta\sigma_{el.}$, $\Delta\varepsilon_{el.}$) as a random variable, with a suitable estimation of its probabilistic distribution, or as a constant term. The random properties of the shrink-fit coupling process would suggest to randomize the state of load, which would be the most correct modeling approach. However, it was observed that the rotor and the CRRs are coupled under very strict tolerances with a severe quality control. With reference to a nominal coupling diameter of about 1150 mm, the mean diametral interference is 2.650 mm (relative interference $\approx$ 0.2%) and may vary between 2.450 mm and 2.850 mm. This careful procedure is justified by the protocol concerning the thermal cycle for CRR swelling and consequent coupling. This is quite a stiff procedure, optimized accounting for the required entity

of interference, the coefficient of thermal expansion of the CRR material and the necessity of preventing any damage to the coils in the rotor slots. Moreover, as the rotor spins, the rotational speed in steady-state conditions is strictly controlled and maintained constant at the aforementioned values. For the listed reasons, it was finally decided to regard the state of load as a deterministic parameter: this is indeed an approximation, but is supported by the remarks in [Zhao (2000)]. This study regards a strain-based fatigue reliability analysis, involving a nuclear reactor material, with specimens machined from a welded pipe and tested under LCF. The whole research is based on the experimental observation of a significant scatter of the cyclic stress-strain responses of the studied material. Its most impressive remarks are the following:

Without considering this scatter, a non-conservative evaluation might be given.

It is important to take the aforementioned scatter into account, as a random cyclic strain applied history can be introduced even under a deterministic loading history. More focus is given on the numerical modeling of this scatter, by determining lower and upper bounds for the cyclic curve and related coefficients, rather than on the modeling of the loading mode and of its random variations.

By comparing the results by [Zhao (2000)] with those of the current research, it can be observed that the studied material also exhibits a not negligible cyclic scattering, and even a (lower) static scattering (Fig. 3). It was consequently decided to consider the slopes and the constant terms of both the static and cyclic curves as random variables with Normal distributions ($U_1, \ldots, U_4$). These variables can be easily associated to the material properties, regarding static and cyclic plasticity and hardening (coefficients K, K', n, n'). This approach makes it possible to model the random properties of the local elasto-plastic stress-strain states, despite the approximation of deterministic loading history.

As previously remarked, the Young's modulus, was considered as a deterministic constant [Wirsching, Torng and Martin (1991), Wu and Wirsching (1984)], with the experimentally determined value of 193.8 GPa [Olmi and Freddi (2010)].

Other four random variables ($U_5, \ldots, U_8$) were associated to the coefficients of the Manson-Coffin model, namely σ'_f, ε'_f, b and c. As previously reported, according to [Wirsching, Torng and Martin (1991), Wu and Wirsching (1984)], Log-Normal distributions were presumed for σ'_f and ε'_f, while Gaussian distributions were considered for the exponents b and c. For the sake of computational efficiency, the variables $Lg(\sigma'_f)$ and $Lg(\varepsilon'_f)$ with Normal distributions were considered. The final remark regards the choice of the output variable. The goal of the probabilistic analysis consisted in the determination of the CDF of the expected life N. Consequently, the device life was chosen as the output variable Y. However, as suggested

in [Wirsching, Torng and Martin (1991), Wu and Wirsching (1984)], a logarithmic scale was adopted. Therefore, $Y = \text{Lg}(N)$ was considered in the analytical computational procedure detailed in Paragraph 2.4.

A resume of the input and output variables is shown in Tab. 1: based on the previous observations, all the variables have Normal distributions, univocally defined by the related mean values (i.e. nominal values resulting by the regression procedure, μ) and standard deviations (*STD*).

Table 1: Input and output random variables

Input random variables		
Variable	Mean value (μ)	Standard Deviation (*STD*)
$U_1 = n$	0.057	0.002
$U_2 = \text{Lg}(K)$	3.001	0.004
$U_3 = n'$	0.052	0.004
$U_4 = \text{Lg}(K')$	2.949	0.010
$U_5 = \text{Lg}(\sigma'_f)$	2.948	0.010
$U_6 = \text{Lg}(\varepsilon'_f)$	-0.830	0.122
$U_7 = b$	-0.043	0.003
$U_8 = c$	-0.546	0.039

Output random variable
$Y = g(\underline{U}) = \text{Lg}(N)$

2.4   Numerical processing for failure probability determination

As previously observed, the AMV, like other similar methods, utilizes a Taylor expansion to achieve a suitable approximation of the function g in the neighbourhood of a MPP, in the coordinates of the multi-dimensional space of the random variables. The computational difficulties arise from the fact that the MPP or design point is initially unknown. Consequently, it must be determined by an iterative method, considering the point defined by the mean values of the random variables as the first expanding point. This procedure consists in the application of the MV-FOSM, when running the first iteration, i.e. the first computation step. The expanding point, is indicated by $[a_1, \ldots, a_r]^T$, or by $\underline{a}$ in compact vector notation. For the sake of generality, r random variables are considered $[U_1, \ldots, U_r]^T$, with $r = 8$ in

the case of the present study.

$$Y(U_1, ..., U_r) = Lg(N)$$

$$= g(\underline{a}) + \left.\frac{\partial g}{\partial U_1}\right|_{(\underline{a})} (U_1 - a_1) + ... + \left.\frac{\partial g}{\partial U_i}\right|_{(\underline{a})} (U_i - a_i) +$$

$$... + \left.\frac{\partial g}{\partial U_r}\right|_{(\underline{a})} (U_r - a_r) + (H.O.T.) \tag{10}$$

$$= g(\underline{a}) + \sum_{i=1}^{r} \left[\left.\frac{\partial g}{\partial U_i}\right|_{(\underline{a})} (U_i - a_i) \right]$$

$$= \alpha_0 + \alpha_1 (U_1 - a_1) + ... + \alpha_i (U_i - a_i) + ... + \alpha_r (U_r - a_r)$$

Eq. 10 shows the first order expansion around the point $\underline{a}$, the term H.O.T. indicates higher order terms that can be neglected. The derivative terms may be easily numerically calculated by the finite difference methods. In particular, the partial derivatives are approximated by quotients of finite differences determined by operating slight perturbations of the random variables around their values at the expanding point. Eq. 11 shows the computation of the (i-th) derivative term, by the forward finite difference approach [Huang and Du (2008)].

$$\left.\frac{\partial g}{\partial U_i}\right|_{(\underline{a})} \approx \frac{\Delta g}{\Delta U_i} = \frac{g(a_1, ..., a_i + \Delta U_i, ..., a_n) - g(a_1, ..., a_i, ..., a_n)}{\acute{a}_i + \Delta U_i - \acute{a}_i} \tag{11}$$

The term ΔU_i in Eq. 11 represents the entity of the (i-th) perturbation: it is theoretically arbitrary, but it must be a good compromise from being too high (would imply a rough estimation of the partial derivative punctual value) and being too low (would imply a very stiff polynomial approximation, being reliable just in a small surrounding of the expanding point). For this purpose, Refs. [Wirsching, Torng and Martin (1991), Wu and Wirsching (1984)] suggest to choose the perturbation size ΔU_i as the 10% of the (i-th) variable standard deviation, i.e. $\Delta U_i = 0,1 \cdot STD(U_i)$. From the operative point of view, the constant term and the derivative ones were determined, by running the mathematical model described in Paragraph 2.2 for nine times. A linear model requires in general $(r + 1)$ runs for the computation of the α_i coefficients in Eq. 10 [Wu and Wirsching (1984)].

The following step consisted in the analytical formulation of the failure function h, Eq. 12. It required the choice of a reference value $y = Lg(N_0)$, where N_0 stands for the number of cycles for which the probability of failure is being computed and can be associated to the life mission. The condition $Lg(N) = Y = y = Lg(N_0)$ represents the limit state at the boundary between failure and service.

$$h(U_1, ..., U_r) = Y(U_1, ..., U_r) - y =$$
$$= \alpha_0 + \alpha_1 (U_1 - a_1) + ... + \alpha_i (U_i - a_i) + ... + \alpha_r (U_r - a_r) - y = 0 \tag{12}$$

It can be observed that a positive value of *h* indicates that the computed life is greater than its reference value, which implies a non failure condition, i.e. no failure occurs in the required life. Whereas, the condition *h* < 0 has the physical meaning of the computed life being lower than the required mission for the turbogenerator rotor, in other words a failure must be expected during turbogenerator use. This is the failure condition, whose probability of occurrence must be estimated. Finally, as previously stated, the condition of *h* = 0, indicates the limit state, where the computed life is exactly equal to the required duration.

The further step consisted in the application of the H-L method to operate variable reduction, i.e. the transformation of the basic variables into the reduced ones. The reduced variables exhibit a Normal distribution with a mean of zero and standard deviation of unity. This procedure was performed according to Eq. 13, where U_i and u_i respectively indicate the (i-th) random variable and the corresponding reduced one.

$$u_i = \frac{U_i - \mu(U_i)}{STD(U_i)} \Leftrightarrow U_i = u_i \cdot STD(U_i) + \mu(U_i) \tag{13}$$

By applying Eq. 13, with the knowledge of the mean values, $\mu(U_i)$, and of the standard deviations, $STD(U_i)$, of each variable U_i (see Tab. 1), all the basic variables in Eq. 12 could be replaced by the related reduced coordinates. This computational procedure may be regarded as a change of the reference system: in the new one the point defined by the mean values of all the input variables is moved to the origin.

Finally, the last step led to the determination of the design point and of its distance from the origin of the new reference system in the reduced variables: this distance is called safety index, β. Computation was performed by solving the following constrained optimization problem.

$$\begin{cases} h(\underline{u}^*) = 0 \\ \beta = \min \|\underline{u}^*\| \end{cases} \tag{14}$$

The symbol * in Eq. 14 indicates the coordinates at the design point: the equations in the constrained system have the following meaning. The design point is univocally determined as the point lying on the failure function (i.e. the limit state between safe and unsafe conditions) that is at the minimum distance from the origin of the reduced reference system. As previously remarked, the origin point corresponds to the condition of all the variables assuming their mean (nominal) values, at the middle of the related Normal distributions.

A graphical interpretation of the failure function separating the safe and unsafe domains, of the properties of the design point and of the conditions expressed by
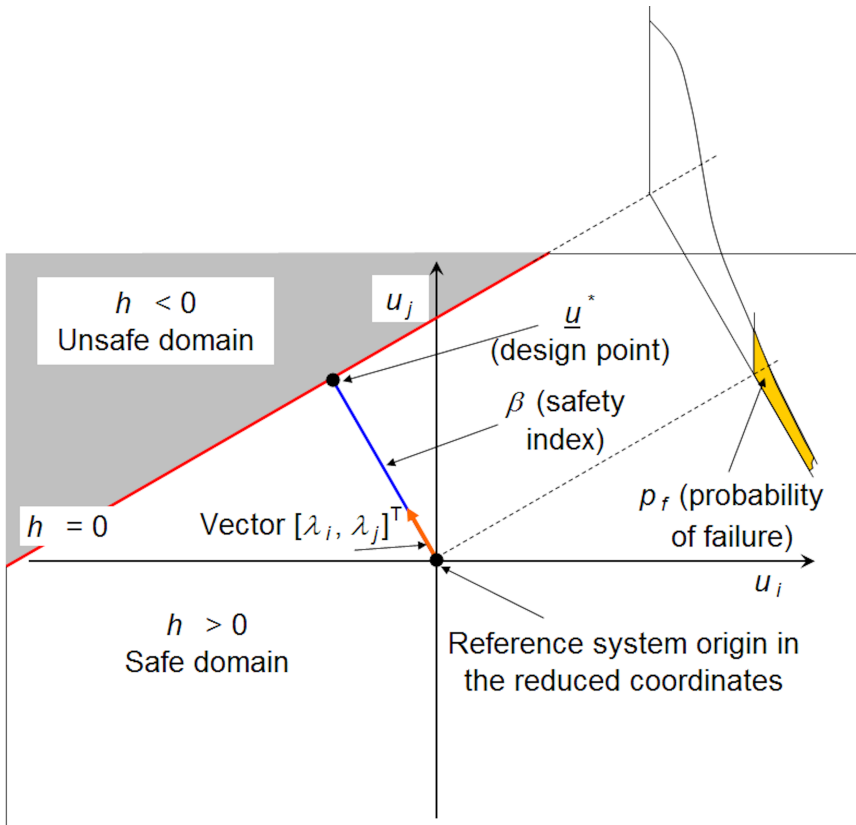
Figure 7: Determination of the design point $\underline{u}^*$, of the safety index β and of the probability of failure p_f in a bi-dimensional reduced coordinate system

Eq. 14, is shown in Fig. 7. For the sake of clearance the graphical representation is sketched in a bi-dimensional reference system $(u_i - u_j)$, while, in reality, the failure function h should be plotted in a r-dimensional space. It can be observed that the design point has the meaning of the most critical point: it corresponds to the values of the random variables which are likely to lead to a failure (lying on the limit state) and are at the same time the closest to the nominal ones (minimum distance from the origin). From the computational point of view, the constrained system was easily solved by the Lagrange multipliers method, by applying the following

equations, Eqs. 15-16.

$$\lambda_i = \frac{\frac{\partial h}{\partial u_i}\bigg|_{\left(\frac{a_1-\mu(U_1)}{STD(U_1)},...,\frac{a_n-\mu(U_n)}{STD(U_n)}\right)}}{\sqrt{\sum\limits_{j=1}^{n}\left(\frac{\partial h}{\partial u_j}\bigg|_{\left(\frac{a_1-\mu(U_1)}{STD(U_1)},...,\frac{a_n-\mu(U_n)}{STD(U_n)}\right)}\right)^2}} \tag{15}$$

$$\underline{u}^* = \beta \cdot [\lambda_1,...,\lambda_i,...,\lambda_n]^T \tag{16}$$

In Eq. 15 the partial derivatives of the failure function h are calculated at the expanding point, here expressed in the reduced coordinates. Its application makes it possible to compute the terms indicated by λ_i, which are the direction cosines of a vector that defines the design point. Subsequently, by applying the relationship in Eq. 16, considering Eq. 14, it is possible to estimate the safety index β and to determine the reduced coordinates of the design point.

The probability of failure p_f is finally calculated by the relationship in Eq. 17, which is based on the hypothesis that the output variable is normally distributed, for being a linear combination of normally distributed input variables. The symbol ϕ in Eq. 17 stands for the standard normal distribution function (see also Fig. 7).

$$p_f = \phi(-\beta) \tag{17}$$

The determined solution is usually regarded as the "Mean value (MV) solution" [Wu, Millwater and Cruse (1990)] and is frequently inaccurate. It can be explained by observing that the probability estimation depends on the determined coordinates of the design point, by Eqs. 14-16. These coordinates, computed by calculating the partial derivatives in Eq. 15, are dependent on the analytical formulations, namely the Taylor expansions, of the functions g and h, Eqs. 10-12. The polynomial expression calculated in Eq. 10 is valid in the neighbourhood of the expanding point, while becomes a poor approximation away. For this reason, in theory, the linear expansion should be performed at the design point, or, at least, the expanding point should be sufficiently close to the design point. However, it is quite frequent, especially when estimating low probabilities of failure, that this condition is not respected and that the finally determined design point is far away from the initially chosen expanding point. Due to the weak approximation, the determined result is not acceptable: the correct one must be determined iteratively, by setting the just determined design point as the new expanding point, and by repeating all the calculation steps, starting from the determination of a new Taylor polynomial expansion. Few iterations usually lead to convergence: in the present case just two were sufficient and, by re-applying Eq. 17, it was finally possible to determine a reliable estimation of the probability of failure p_f.

In order to determine the whole CDF, in the life duration of the studied machine, different values of N_0 were considered, in the range from some thousands to 30,000. The computational procedure described above was therefore repeated for different values of N_0 in the specified range. This approach appears to be more accurate than that described in some references, e.g. in [Wu and Wirsching (1984)]. The methodology there described, studied by Wu in the development of the AMV method, made use of the same polynomial fit for the simultaneous estimation of several design points and probability of failures, each corresponding to a different value of N_0. The iterative calculation was performed by choosing the new expanding point as an average of the determined design points.

The computation of the CDF of the rotor life was completed by an additional MC simulation. It was performed at a high number of iterations, $5 \cdot 10^6$, and its results were compared to the previously obtained yields, in order to make a comparative analysis, also in terms of computational efficiency.
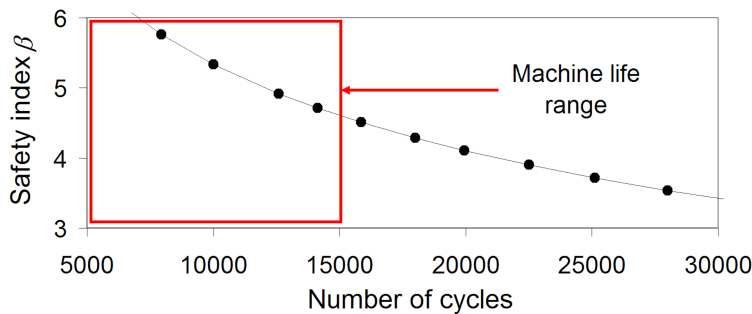

Figure 8: Determination of the safety index β in the machine life range

3 Results and Discussion

Figs. 8-9 show the obtained results in terms of the safety index and of the probability of failure: the yields are plotted in a life interval up to 30,000 loops, while the usual machine life range, up to 15,000 cycles, is highlighted. The two cumulative distribution functions, obtained by numerical iteration and by MC simulation are plotted together in Fig. 9.

Dealing first with safety index results, it can be remarked that β assumes values higher than 4 in the whole machine life range. This amount can be compared to that reported by [Avrithi and Ayyub (2010)] as a reference value: Avrithi and Ayyub (2010) dealt with their involvement in the probabilistic design of nuclear pipes by the AFOSM method. Based on the literature in the field, they set the target
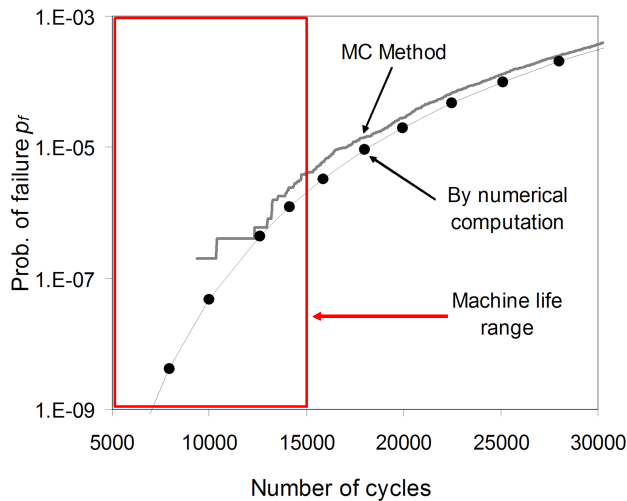
Figure 9: Determination of the probability of failure p_f in the machine life range and result validation by comparison with the simulated curve by MC

reliability index (minimum desired value) to 3. In other contributions, in particular in [ENV 1991-1 (1994); Mansour, Wirsching, White and Ayyub (1992)], safety index reference ranges are reported for the fatigue design of different structures. For instance, in the case of buildings or bridges, the suggested interval is between 1.5 and 3.8, while in ship design the target safety index is usually between 2 and 3.5. This comparative analysis leads to the conclusion that the obtained values are all well consistent with the reference values in the current literature and therefore acceptable to achieve the reliability requirements.

The second point of discussion regards the computational efficiency of the here applied probabilistic numerical method. The MC simulation took about 35 hours for the completion of $5 \cdot 10^6$ iterations, moreover, as remarked in several references, e.g. in [Huang and Du (2008)], it was suitable to estimate probabilities greater than 10^{-6} and, at a rough approximation, probabilities down to $2 \cdot 10^{-7}$. Despite the long computational time, MC was inefficient to estimate probabilities lower than the $2 \cdot 10^{-7}$ threshold, as it would have required additional iterations. This result shows that the MC method is highly expensive and extremely inefficient in the estimation of probability of failures in the investigated range. The numerical method was implemented in the Matlab environment (release 7.9.0.529 (R2009b)). The dot results indicated in Figs. 7-8 were obtained by running a Matlab routine with built-in automatic iterative calculation up to result convergence. The proce-

dure was repeated several times, one for each of the N_0 values. An important issue to remark is that the proposed linear algorithm is very efficient: just two iterations were usually sufficient for result convergence: the corresponding computational time resulted to be remarkably short, in the order of 10 s. This good efficiency was maintained even when estimating very low probabilities, lower than 10^{-7}, at different turbogenerator life stages. The numerical procedure was applied to determine probabilities in a quite wide life range, up to 30,000 cycles, beyond the typical turbogenerator life, in order to make a comparison with MC results. Fig. 9 shows a good agreement between the two CDFs, even if the resolution of the MC curve tends to become poor, as the probability of failure becomes lower than 10^{-6}. From the quantitative point of view, the estimated probability of failure is about $3 \cdot 10^{-10}$ after 6,000 loops, $4 \cdot 10^{-9}$ at 7,900 loops and increases up to $5 \cdot 10^{-8}$ after 10,000 loops and to $3 \cdot 10^{-6}$ at 15.000 loops, i.e. at the end of the turbogenerator fifty-year life. This values are in the typical order of magnitude of the probability of failure of highly loaded components under LCF, whose breakage may have very serious consequences. For example, the study in [Liu, Lu, Xu and Yue (2005)] deals with the probabilistic analysis of an aeronautical engine turbine disc structure, which leads to the estimation of the highest probability of failure at the most loaded section, in the order of 10^{-8}.

As previously reported, in [Zhao (2000)] it is emphasized that failing to consider the scatter in the component cyclic stress-strain response may lead to a non-conservative evaluation of the probability of failure. A confirmation of this remark arises from the comparison of the results in Fig. 9 with those contained in [Bendandi (2010)]. This Ref. regards a preliminary study supervised by the author, where just 4 (instead of 8) random variables had been considered: these 4 variables were related to the 4 parameters of the Manson-Coffin model, while the coefficients of plasticity and the hardening exponents had been regarded as deterministic parameters. The simplified model underestimated the failure probability in the order of 35% at the end of the machine life, while the differences were much greater, up to one order of magnitude, at the previous stages of the machine life.

4   Conclusions

The present paper was developed in a research programme aimed at the LCF design of turbogenerator rotors and CRRs. At the first stages, the topic was approached from the experimental point of view, by the lab characterization of the mostly used materials for the manufacturing of the aforementioned components [Olmi and Freddi (2009)]. The following step regarded the use of experimental data and of the load spectra for design purposes: a deterministic approach was initially adopted in the analysis [Olmi and Freddi (2010)]. The subject of the present study was also

concerned with the use of the experimental data for improving design, but this goal was fulfilled from the probabilistic point of view, with a detailed analysis on how to interface the experimental outputs with the development of a reliability method and the determination of probabilistic data. In particular, focus was given on the computation of the probability of failure at the most critical section, the shrink-fit zone of the rotor.

The main important points, related to the applied methodology and the obtained results, can be so summarized:

The analysis of the literature in the field of turbogenerators showed that there are few papers dealing with the fatigue properties of the involved materials. Moreover, studies relating the LCF material experimentation to the determination of the probability of failure at the most critical locations are missing.

The final goal of the reliability analysis usually consists in the determination of the CDF of the output variable (in this case: the rotor life). The conventional approaches, i.e. the calculation of the integral of the joint probability density function or the MC method, are extremely expensive and inefficient in the estimation of low probabilities. Alternative numerical methods are available, for instance the AMV [Wu, Millwater and Cruse (1990)], even if a detailed description of all the analytical steps for probability computation is often missing.

It was shown how, from experimental data regarding the static, cyclic and LCF curves of the studied material, it is possible to determine the coefficients for their mathematical formulation and to individuate random variables related to these parameters. A suitable statistic method was applied to estimate their standard deviations from data scattering and to finally determine their probabilistic distributions.

The probabilistic analysis considered 8 random variables, related to the static and cyclic coefficients of plasticity and hardening exponents and to the fatigue strength and ductility coefficients and related exponents. The nominal state of load was presumed to be deterministic, but this choice was supported by design and assembly issues and by current literature [Zhao (2000)], which recommended the consideration of the scatter of the local static and cyclic stress-strain response.

The applied numerical method is highly accurate and efficient in comparison with the more conventional MC method. The CDF of the rotor life could be determined in a short computational time, about 400 times lower than that required by a MC simulation with $5 \cdot 10^6$ iterations.

The computational time is due to the reduced number of coefficient estimations (namely, the derivative coefficients of the polynomial expansion) to be performed in the probability computation. In the present case each estimation consisted in the simulation of the static curve and of the hysteresis loops, in the determination

of the local stress-strain states and in the estimation of the life, by the Manson-Coffin (modified Morrow approach) and Palmgren-Miner models. Moreover, the procedure was repeated just twice, as two iterations were sufficient for result convergence.

The efficiency is as greater as more complicated are the numerical computations, which should be iterated for a very high number of times by a conventional MC simulation.

The applied method, in the proposed formulation may be extended to many other engineering applications. For instance, in the turbogenerator field, it can be used for the probabilistic computation of CRRs and of copper connectors. Other possible applications regard turbine disks [Liu, Lu, Xu and Yue (2005)] or blades [Vyas, Sidharth and Rao (1997)], or piping systems [Zhao (2000); Avrithi and Ayyub (2010)]. Moreover, in [Wirsching, Torng and Martin (1991)] an interesting application to fracture mechanics is suggested. The described method was successfully applied in a probabilistic study of residual life, considering a long crack propagating in a press column [Olmi (2011)].

The numerical results show that in the typical turbogenerator life range the safety index is higher than 4, while the related probability of failure varies from 4 cases out of one milliard at half life, to 5 cases out of one hundred million after 10,000 cycles and to 3 cases out of one million at full life. The numerical approach made it possible to easily estimate even very low probabilities, providing data that MC simulations are extremely inefficient to process. All the results are fully consistent with reference values in the scientific and technical literature.

References

Apostolakis, G. (1990): The concept of probability in safety assessments of technological systems. *Science*, vol. 250, no. 4986, pp. 1359–1364.

ASM International Handbook Committee (1996): *ASM Handbook Volume 19: Fatigue and Fracture*. ASM International.

Avrithi, K.; Ayyub, B. M. (2010): A Reliability-Based Approach for Low-Cycle Fatigue Design of Class 2 and 3 Nuclear Piping. *Journal of Pressure Vessel Technology*, vol. 132, pp. 051202-1–6.

Balitskii, A.; Krohmalny, O.; Ripey, I. (2000): Hydrogen cooling of turbogenerators and the problem of rotor retaining ring materials degradation. *Int J Hydrog Energy*, vol. 25, pp. 167–171.

Bannantine, J. A.; Comer, J. J.; Handrock, J. L. (1990): *Fundamentals of metal fatigue analysis*. Prentice-Hall.

Bendandi, R. (2010): *Utilizzo di metodi probabilistici nella progettazione a fatica oligociclica di un rotore per turboalternatore*. Bachelor Degree Thesis, Mechanical Engineering, Engineering Faculty, University of Bologna, Tutor: Olmi, G..

Breitung, K. (1984): Asymptotic approximations for multinomial integrals. *Journal of Engineering Mechanics*, vol. 110, no. 3, pp. 357–367.

Che, Y. (2008): *Aging structure life prediction and reliability assessment*. Master's Thesis, School of Aerospace, Mechanical and Manufacturing Engineering, RMIT University.

Cornell, C. A. (1969): A probability based structural code. *J. Am. Concr. Insf.*, vol. 66, pp. 974–985.

Dowling, N. E. (2006): *Mechanical Behavior of Materials (3rd edition)*. Prentice-Hall.

Doyle, J. F. (2004): *Modern Experimental Stress Analysis*. West Sussex, England, John Wiley and Sons Ltd..

Du, X.; Chen, W. (2004): Sequential optimization and reliability assessment for probabilistic design. *ASME Journal of Mechanical Design*, vol. 126, no. 2, pp. 225–233.

Du, X.; Chen, W. (2000): Towards a better understanding of modeling feasibility robustness in engineering design. *ASME Journal of Mechanical Design*, vol. 122, no. 4, pp. 385–394.

Du, X.; Sudjianto; A.; Chen, W. (2004): An integrated framework for optimization under uncertainty using inverse reliability strategy. *ASME Journal of Mechanical Design*, vol. 124, no. 4, pp. 562–570.

Ebbeler, D. H.; Newlin, L. E.; Grigoriu, M. (1995): Alternative computational approaches for probabilistic fatigue analysis. In: *Proc. 36th AIAA/ASME/ASCE Conference on Structures, Structural Dynamics and Materials*, Section on Probabilistic Applications, New Orleans.

Ellyin, F. (1997): *Fatigue Damage, Crack Growth and Life Prediction*. Chapman & Hall.

ENV 1991-1 (Eurocode 1) (1994): *Basis of design and actions on structures - Part I: Basis of design*. CEN (Comite Europien de la Normalisation), Brussels.

Haldar, A.; Mahadevan, S. (2001): *Probability, reliability, and statistical methods in engineering design*. Wiley.

Hasofer, A. M.; Lind, N. C. (1974): Exact and invariant second-moment code formal. *Journal of Engineering Mechanics Div. ASCE*, vol. 100 (EM1), pp. 111–121.

Hohenbichler, M.; Gollwitzer, S.; Kruse, W.; Rackwitz, R. (1987): New light on first- and second-order reliability methods. *Structural Safety*, vol. 4, pp. 267–284.

Huang, B.; Du, X. (2008): Probabilistic uncertainty analysis by mean-value first order Saddlepoint Approximation. *Reliability Engineering and System Safety*, vol. 93, pp. 325–336.

ISO 12106 (2003): *Metallic materials – Fatigue testing – Axial-strain-controlled method*.

Kilpatrick, N. L.; Schneider, M. I. (1988): Update on experience with in-service examination of non-magnetic rings on generator rotors. In: Proc. of the Generator Retaining-Ring Workshop (EPRI-EL-5825), Charlotte, North Carolina, USA, 15-17 September, 1987, pp. 103-109.

Liu, C. L.; Lu, Z. Z.; Xu, Y. L.; Yue, Z. F. (2005): Reliability analysis for low cycle fatigue life of the aeronautical engine turbine disc structure under random environment. *Materials Science and Engineering A*, vol. 395, pp. 218–225.

Mailhot, A.; Villeneuve, J. P. (2003): Mean-value second-order uncertainty analysis method: application to water quality modeling. *Advances in Water Resources*, vol. 26, no. 5, pp. 491–499.

Mansour, A. E.; Wirsching, P. H.; White, G. J.; Ayyub, B. M. (1992): *Probability-Based Ship Design: Implementation of Design Guidelines*. NTIS, Washington, DC, Report No. SSC 392.

Nikolaidis, E.; Chen, S.; Cudney, H.; Hatftka, R. T.; Rosca, R. (2004): Comparison of probability and possibility for design against catastrophic failure under uncertainty. *ASME Journal of Mechanical Design*, vol. 126, no. 3, pp. 386–394.

Olmi, G. (2012): Low Cycle Fatigue experiments on turbogenerator steels and a new method for defining confidence bands. *Journal of Testing and Evaluation (JTE)*, vol. 40, no. 4.

Olmi, G. (2011): Utilizzo di metodi non lineari nella valutazione affidabilistica di dispositivi meccanici con più variabili aleatorie. In: *Proc. 40th AIAS National Conference*, Palermo, Italy.

Olmi, G.; Freddi, A. (2009): Fatica oligociclica di cappe e rotori di turboalternatori: progetto e costruzione di attrezzatura e prime prove sperimentali. In: *Proc. XXXVIII AIAS National Conference*, Torino, Italy.

Olmi, G.; Freddi, A. (2010): Fatica oligociclica su cappe e rotori di turboalternatori: prove sperimentali, valutazione dell'anisotropia dei materiali, analisi di sensitività sui modelli di comportamento. In: *Proc. XXXIX AIAS National Conference*, Maratea, Italy.

Olmi, G.; Freddi, A. (2010): LCF on turbogenerator rotors and coil retaining

rings: material characterization and sensitivity analyses. In: *Proc. ICEM14 (14th International Conference on Experimental Mechanics)*, Poitiers, France, pp. 42006-1–9.

Orita, K.; Ikeda, Y.; Iwadate, T.; Ishizaka, J. (1990): Development and production of 18Mn-18Cr non-magnetic retaining ring with high yield strength. *ISIJ J*, vol. 30, pp. 587–593.

Putko, M. M.; Newman, P. A.; Taylor III, A. C.; Green, L. L. (2002): Approach for uncertainty propagation and robust design in CFD using sensitivity derivatives. *ASME Journal of Fluids Engineering*, vol. 124, no. 1, pp. 60–69.

Rackwitz, R.; Fiessler, B. (1978): Structural reliability under combined load sequences. *Computers & Structures*, vol. 9, pp. 489–494.

Seo, H. S.; Kwak, B. M. (2002): Efficient statistical tolerance analysis for general distributions using three-point information. *International Journal of Production Research*, vol. 40, no. 4, pp. 931–944.

Skorchelletty, V. V.; Silina, E. P.; Zaytsev, V. A.; Maslov, V. V.; Lubeznova, T. D. (1981): Stress corrosion cracking of turbogenerators rotors retaining rings. *Elektrychiskie stantsii*, vol. 12, pp. 40–42.

Speidel, M. O. (1981): Nichtmagnetisierbare stahle fur generator-kappenringe, ihr widerstand gegen korrosionermundung. *VGB Kraftwerkstechnik*, vol. 61, no. 5, pp. 1048–1053.

Suresh, S. (1991): *Fatigue of Materials*. Camb Univ Press, Cambridge, UK.

Thoft-Christensen, P.; Baker, M. J. (1982): *Structural reliability theory and its application*. Berlin, Heidelberg, New York, Springer.

Vyas, N. S.; Sidharth; Rao, J. S. (1997): Dynamic stress analysis and a fracture mechanics approach to life prediction of turbine blades. *Mechanism and Machine Theory*, vol. 32, no. 4, pp. 511–527.

Wang, L.; Grandhi, R. V. (1996): Safety index calculation using intervening variables for structural reliability analysis. *Computers & Structures*, vol. 59, no. 6, pp. 1139–1148.

Wirsching, P. H.; Torng, T. Y.; Martin, W. S. (1991): Advanced fatigue reliability analysis. *International Journal of Fatigue*, vol. 13, no. 5, pp. 389–394.

Wu, Y. T.; Millwater, H. R.; Cruse, T. A. (1990): Advanced probabilistic structural analysis method for implicit performance functions. *AIAA Journal*, vol. 28, no. 9, pp. 1663–1669.

Wu, Y. T.; Wirsching, P. H. (1984): Advanced Reliability Method for Fatigue Analysis. *Journal of Engineering Mechanics*, vol. 110, no. 4, pp. 536–553.

Youn, B. D.; Choi, K. K. (2004): An investigation of nonlinearity of reliability based design optimization approaches. *ASME Journal of Mechanical Design*, vol. 126, no. 3, pp. 403–411.

Youn, B. D.; Choi; K. K. (2004): Selecting probabilistic approaches for reliability-based design optimization. *AIAA Journal*, vol. 42, no. 1, pp. 124–131.

Zhao, Y. X. (2000): A methodology for strain-based fatigue reliability analysis. *Reliability Engineering and System Safety*, vol. 70, pp. 205–213.